Secondary Electron-Positron Pairs as a Key Component of the Solar Disk TeV Emission

Wenyu Cao[1]、Chingam Fong[1]、Zhe Li[2]、Kenny Chun Yu Ng[1]

1 The Chinese University of Hong Kong

2 Institute of High Energy Physics, CAS

2026.9.2

Outline

- Motivation & Background
  - The magnetic field plays a crucial role
  - The electron–positron signal is indistinguishable from gamma rays
  - TeV observations of solar gamma rays
- G4Solar Simulation
  - G4Solar
  - Simulation Setup
  - Response Matrix
- Results
  - The ratio of $e^{\pm}$
  - Morphology

The magnetic field plays a crucial role

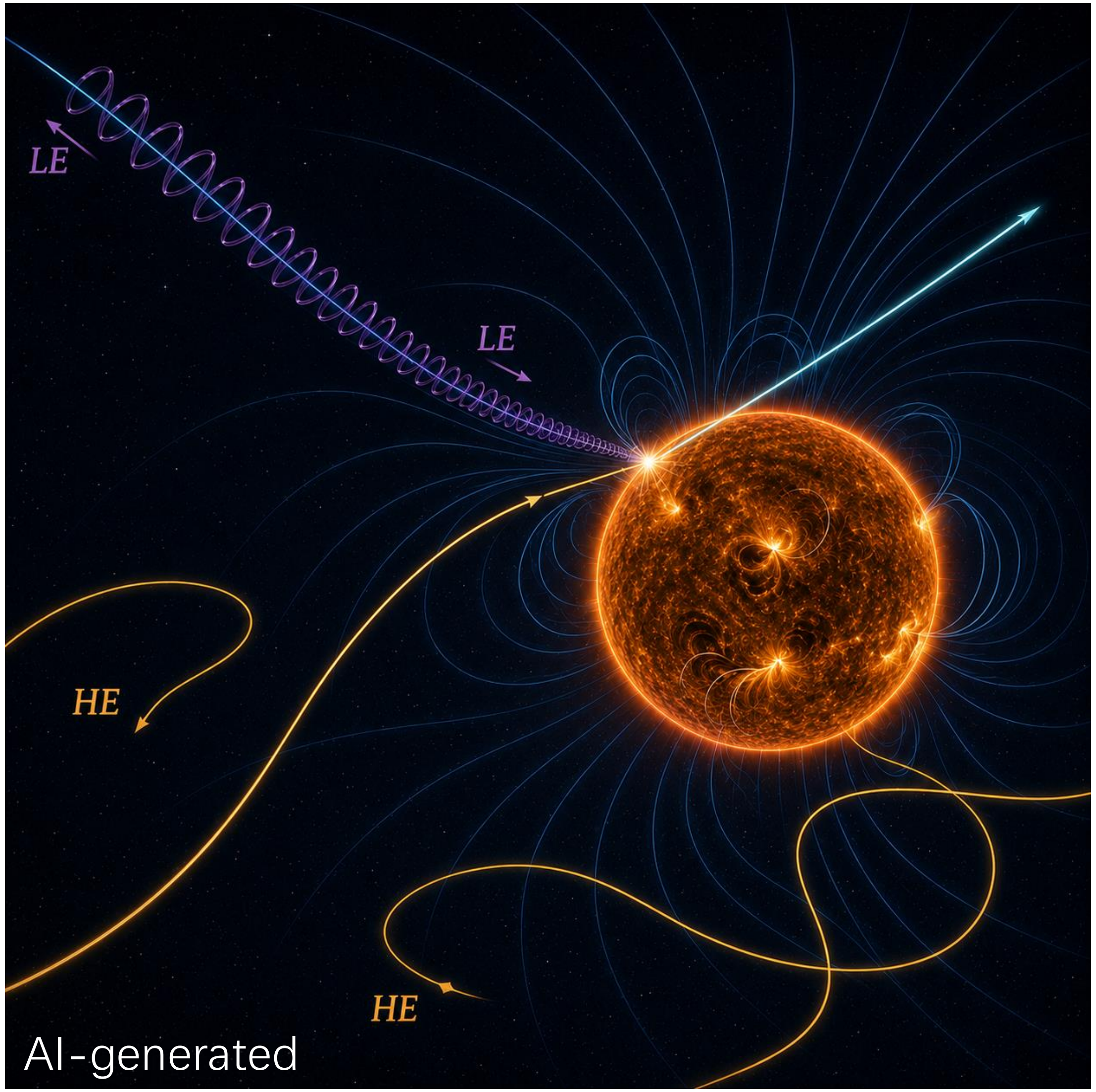

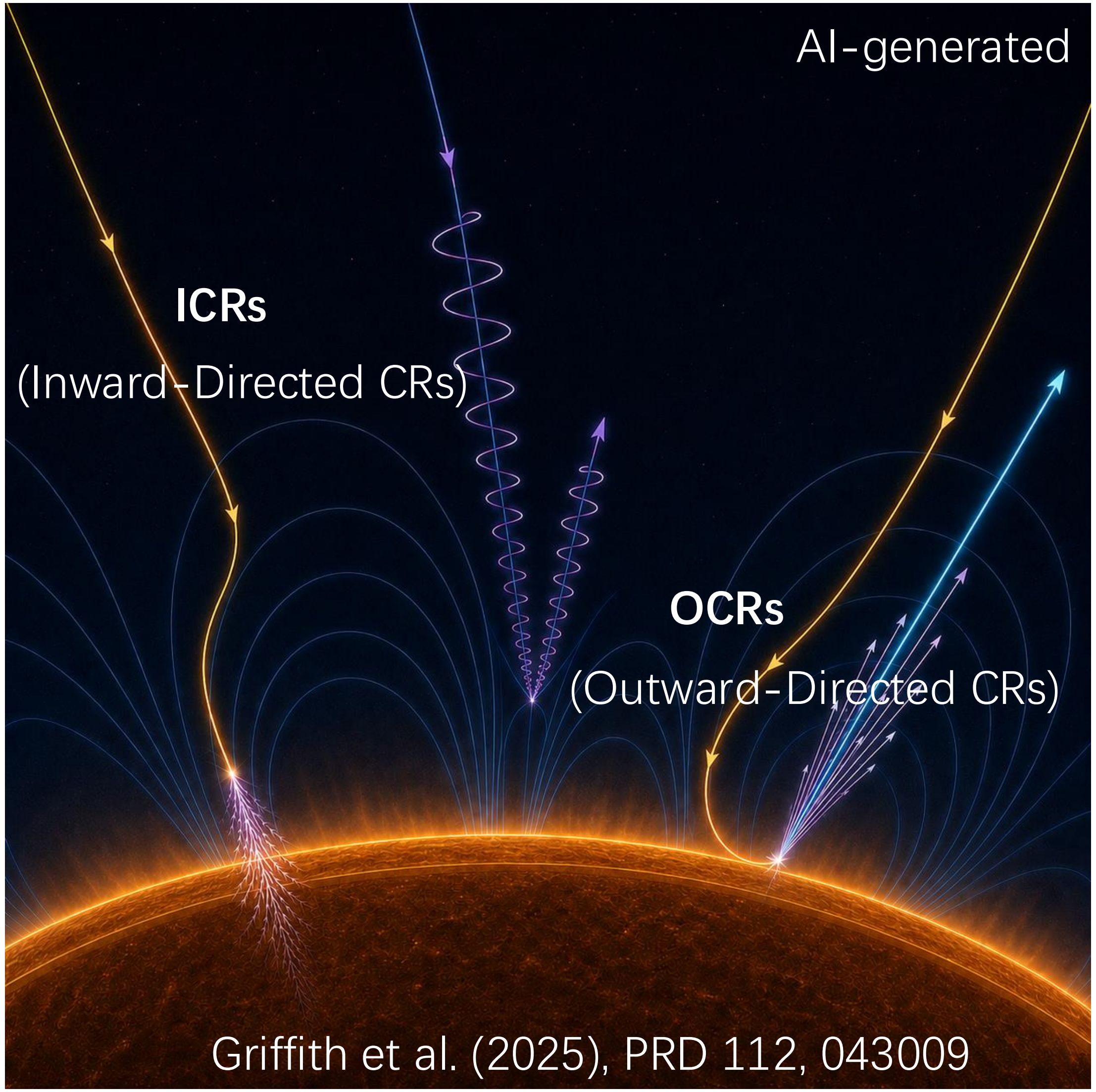

The electron–positron signal is indistinguishable from gamma rays

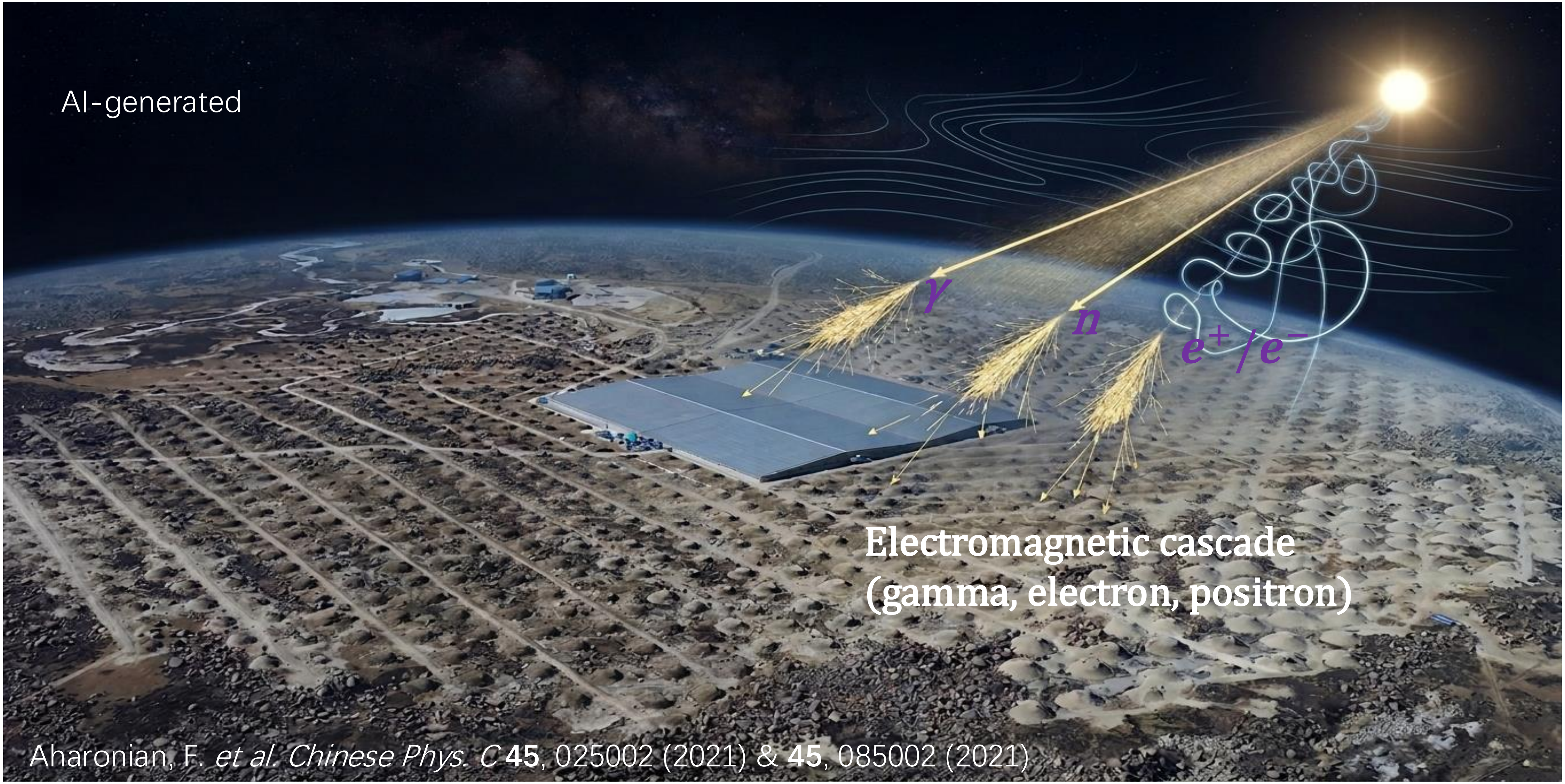

TeV observations of solar gamma rays

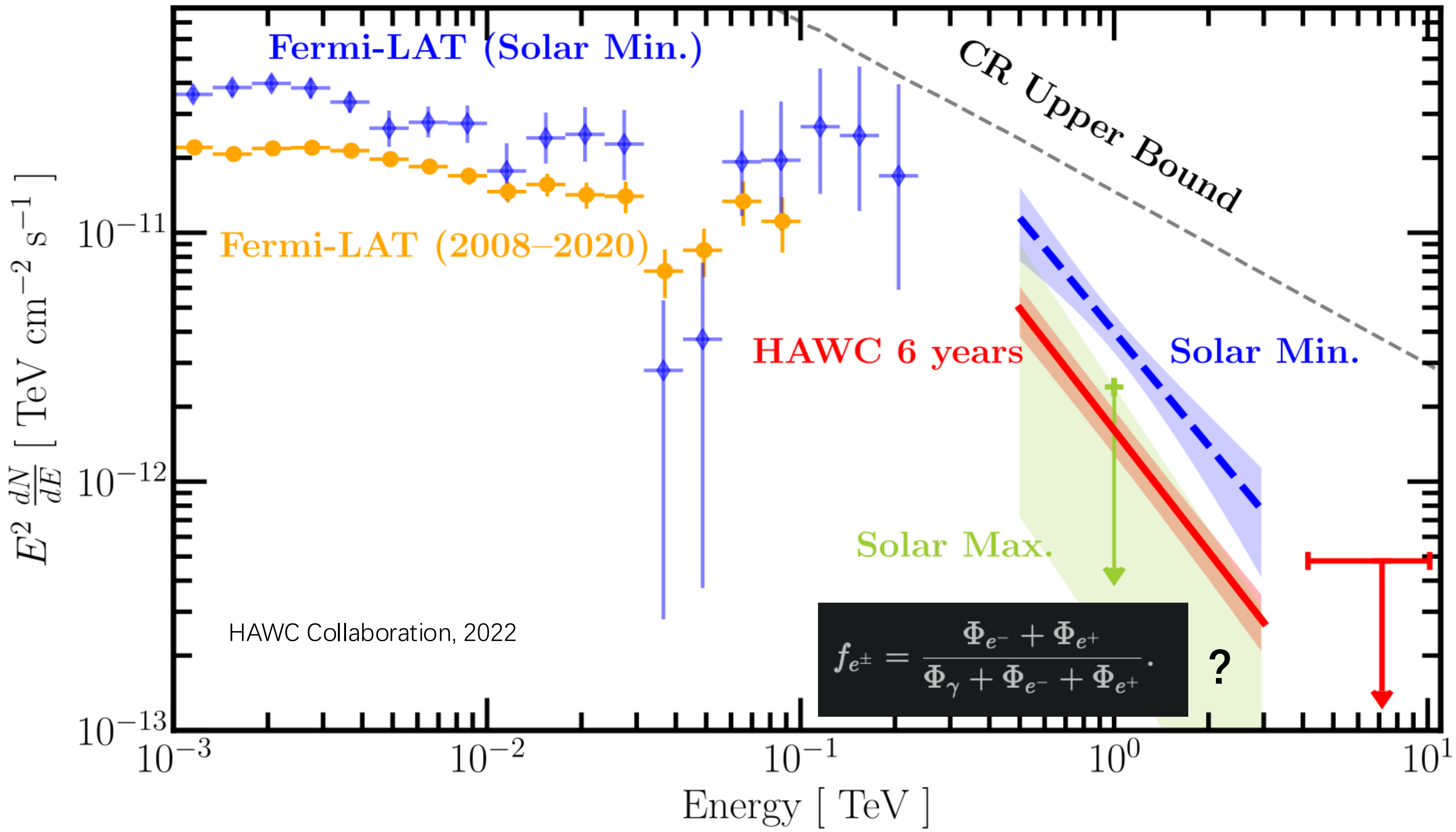

Phys. Rev. Lett. **131**, 051201, HAWC Collaboration

G4Solar

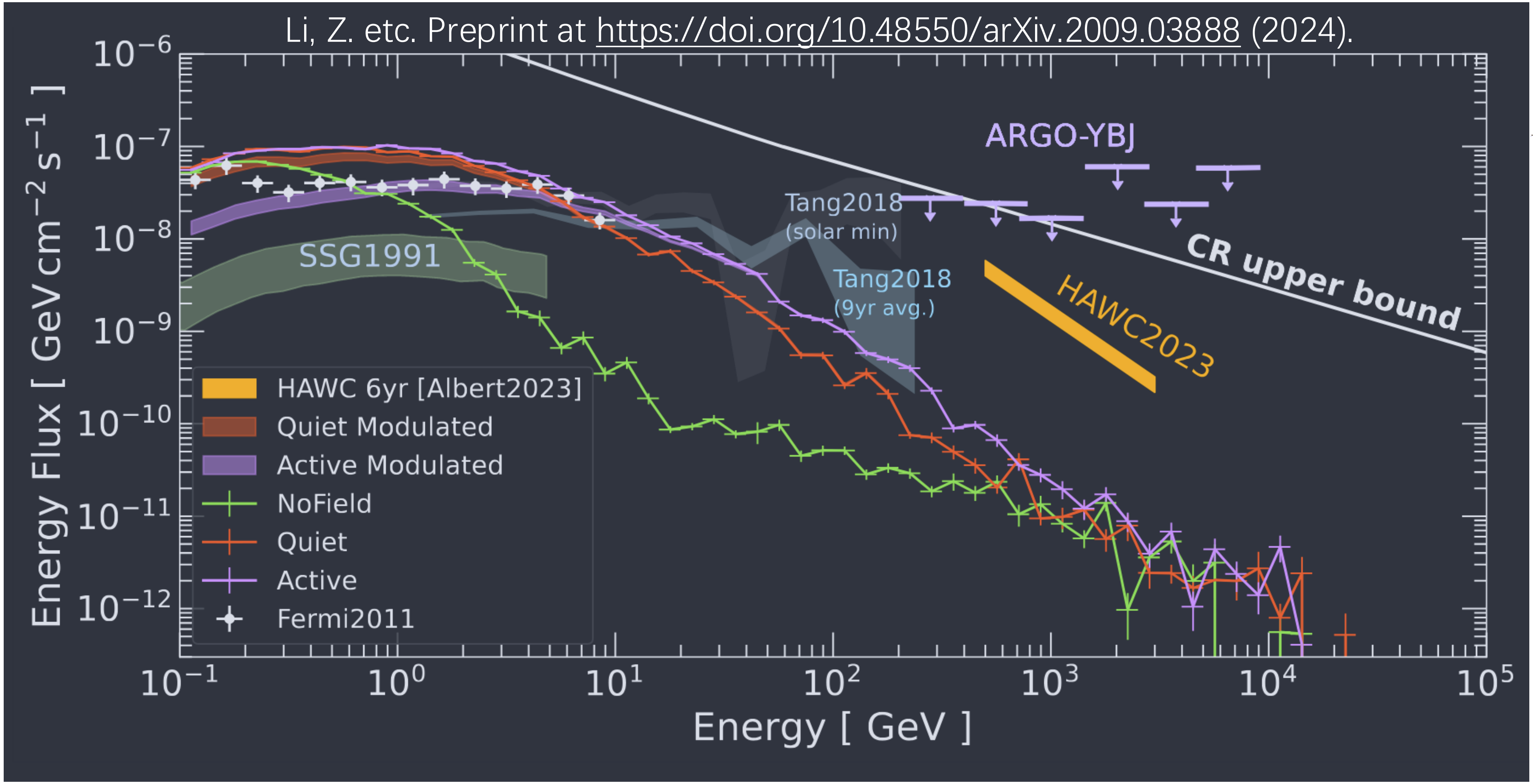

GEANT4
A SIMULATION TOOLKIT

G4SOLAR

developed by Li Zhe, arXiv:2009.03888v2

G4Solar Simulation

GEANT4
A SIMULATION TOOLKIT

G4SOLAR

developed by Li Zhe,
arXiv:2009.03888v2

Main Assumptions:

CR are deflected by the B field and emitted outward from a specific **Depth** within the Sun with a specific **Spectrum** and **Angular Distribution.** We refer to such cosmic rays as **Outward CRs (OCRs).**

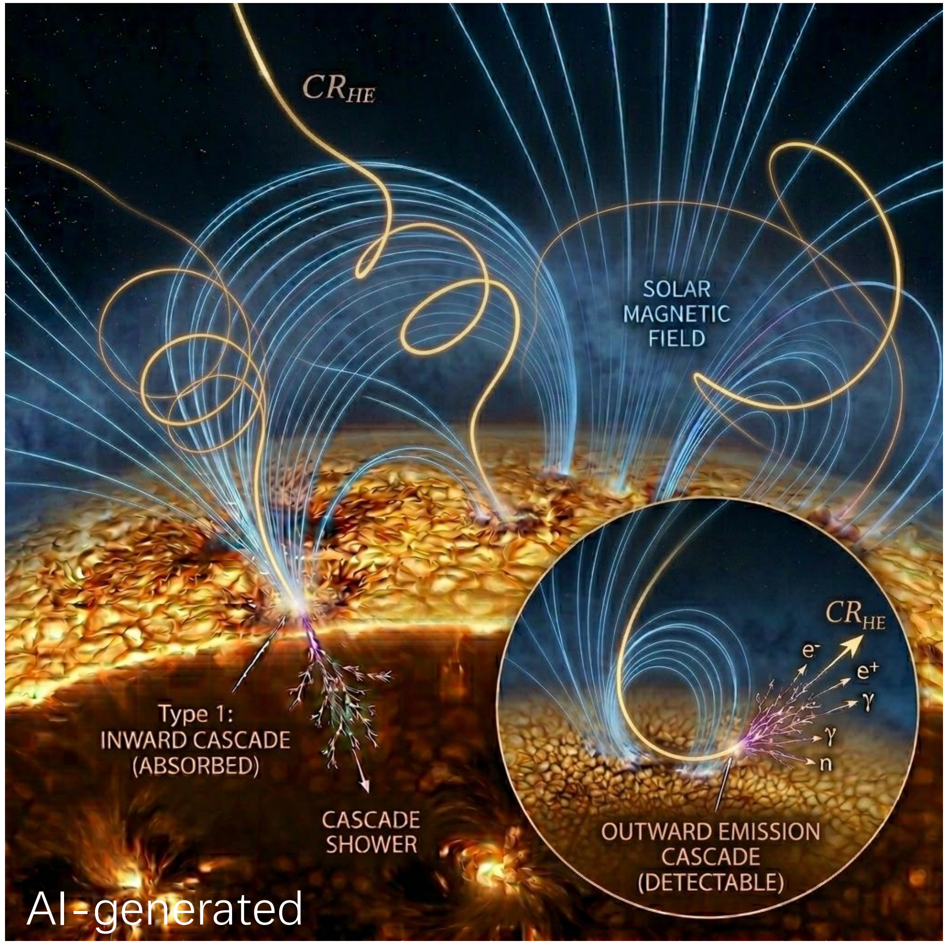

Injection Energy Spectrum:

$$\Phi_{\mathrm{OCR}}(E_p) = A\left(\frac{E_p}{E_0}\right)^{-\gamma} \exp\left(-\frac{E_p}{E_{\mathrm{cut}}}\right)$$

The Outward CR He spectrum is derived from the observed He/p ratio in the rigidity spectrum.

Injection Depth:

$[R_\odot - 2000km, R_\odot + 2000km]$
(Uniform distribution、etc.)

Injection Angular Distribution:

Radial、Isotropic、Lambertian、Sinusoidal、Tangent、etc.

G4Solar Simulation

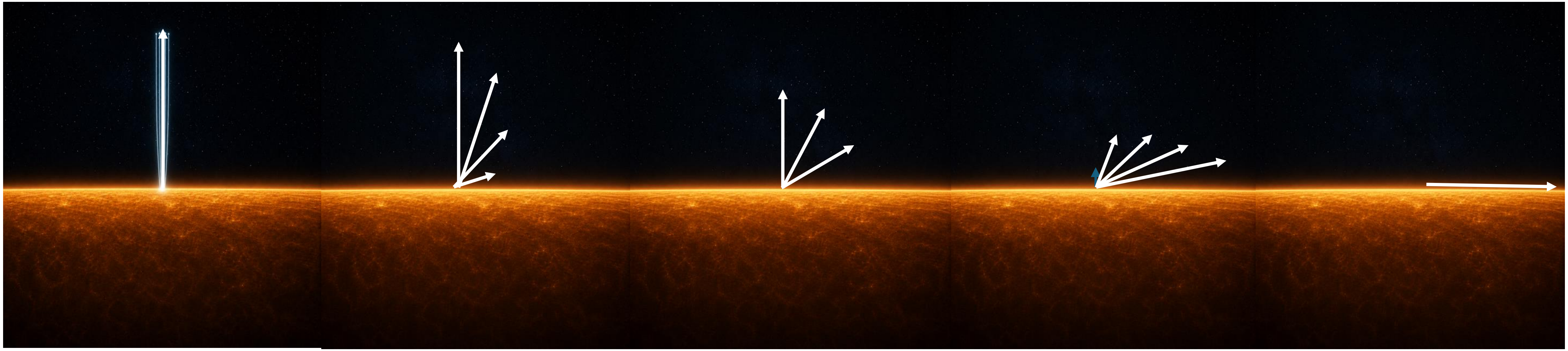

Radial	Lambertian	Isotropic	Sinusoidal	Tangent
$\theta = 0^{\circ}$	$f(\theta) \sim \cos(\theta)$	$f(\theta) \sim \mathrm{const}$	$f(\theta) \sim sin(\theta)$	$f(\theta) \sim 90^{\circ}$

More radial → More tangent

Solar Response Matrices

Solar Response $\boldsymbol{Y(E_i|E_p)}$

$$Y(E_i|E_p) = \frac{dN_i}{dE_i}(E_i|E_p) = \frac{N_i(E_i|E_p)}{N_{\rm inj}(E_p)\Delta E_i}.$$

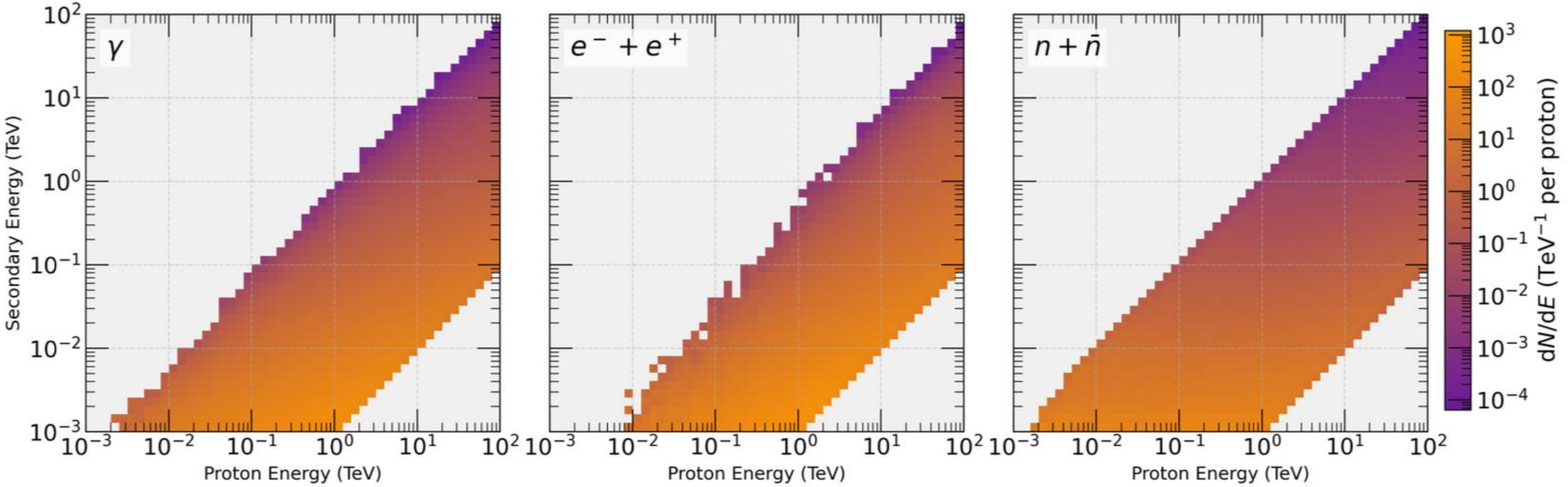

the response to the He nucleus was also simulated: $\boldsymbol{Y(E_i|E_\alpha)}$

χ^2 Fitting

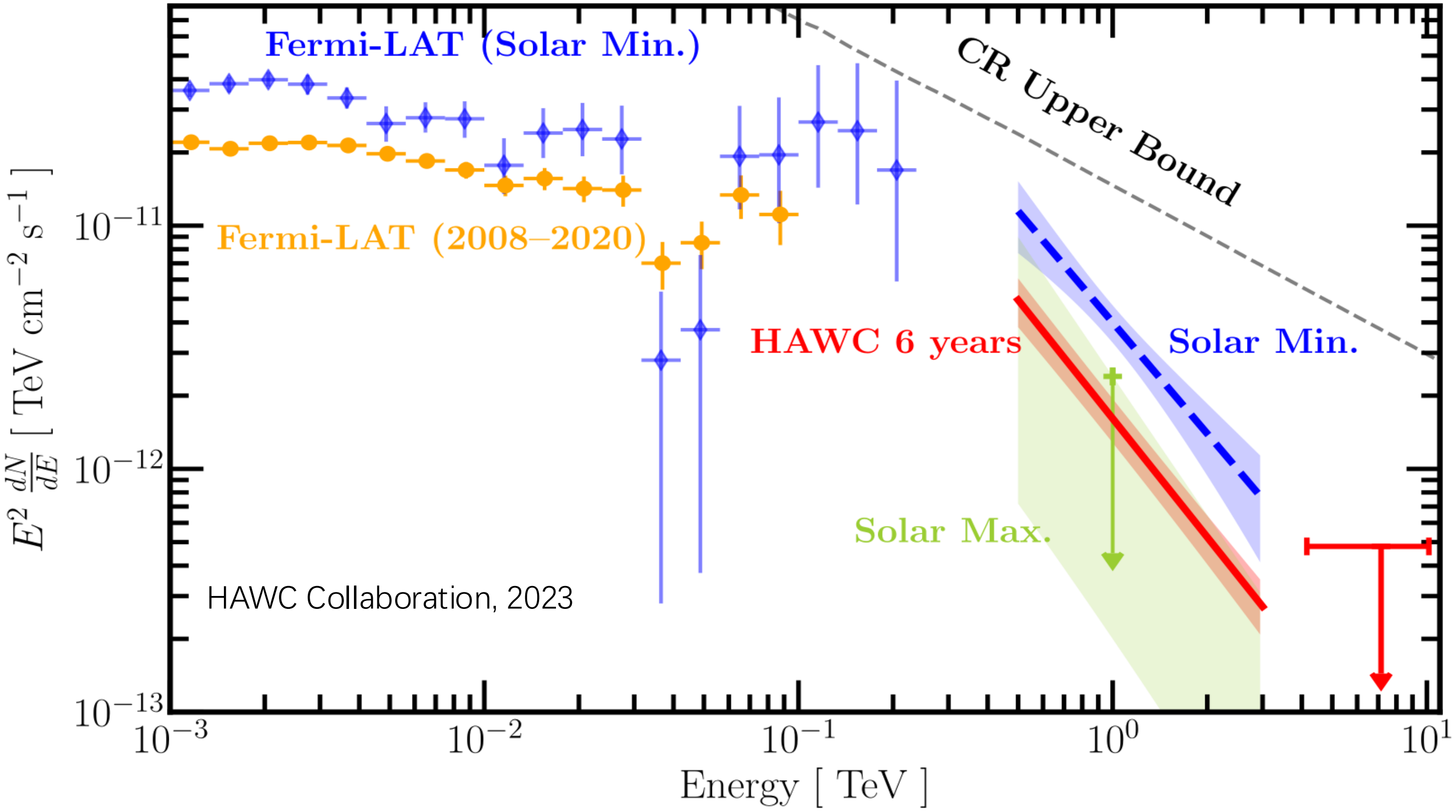

Phys. Rev. Lett. **131**, 051201, HAWC Collaboration

- Calculate the expected fluxes of secondary particles received at Earth

$$F_{\mathrm{simu},i}(E_i) = \int dE_p\, Y(E_i|E_p) \times \pi\Phi_{\mathrm{OCR}}(E_p) \cdot \frac{4\pi R_{\mathrm{inj}}^2}{\Omega_{\mathrm{band}} R_{\mathrm{obs}}^2},$$

- Fit them to the Fermi (γ) and HAWC (γ+$e^{\pm}$) observations

$$F_{\mathrm{simu},k}(E) = \begin{cases} F_\gamma(E), & k = \text{Fermi-LAT} \\ F_\gamma(E) + F_{e^+}(E) + F_{e^-}(E), & k = \text{HAWC} \end{cases}$$

$$\chi^2 = \sum_{k\in\mathcal{D}} \sum_{j=1}^{N_k} \frac{(F_{\mathrm{simu},k}(E_j) - F_{\mathrm{obs},k}(E_j))^2}{\sigma^2_{\mathrm{stat},k,j} + \sigma^2_{\mathrm{simu},k,j} + (e_{\mathrm{sys}} F_{\mathrm{obs},k}(E_j))^2},$$

Parameter space and systematic uncertainties

Fit each hypothesis separately.

Selection Criteria:

$$\chi^2_{\rm red} = \chi^2/{\rm dof} \leq 2$$

$$\Phi_{p,\rm OCR}(E) \leq \Phi_{p,\rm GCR}(E)$$

- The deeper the injection and the more tangential the direction, the larger the $e^{\pm}$ fraction.
- Too shallow: insufficient interactions; too deep: excessive gamma absorption.

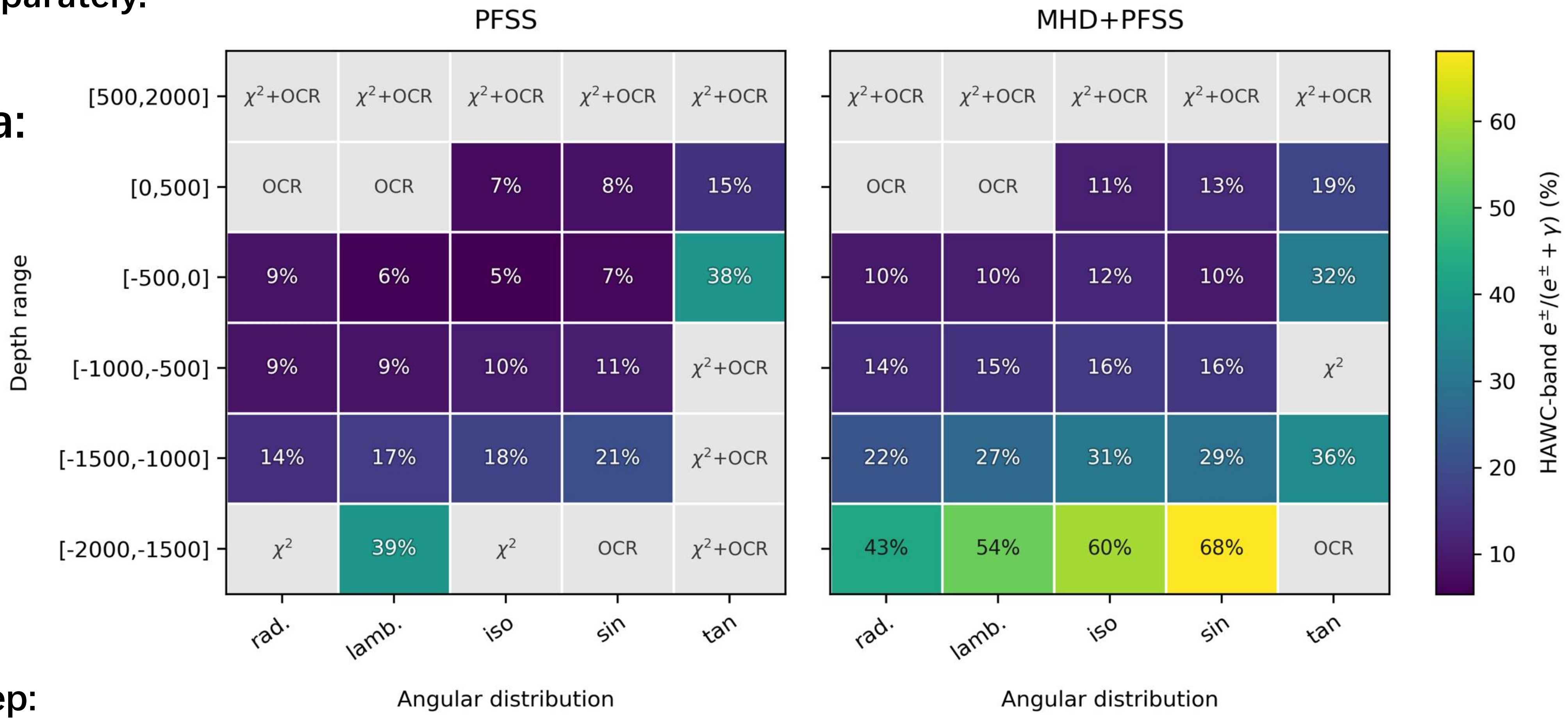

38 physically allowed models

Fitting Results

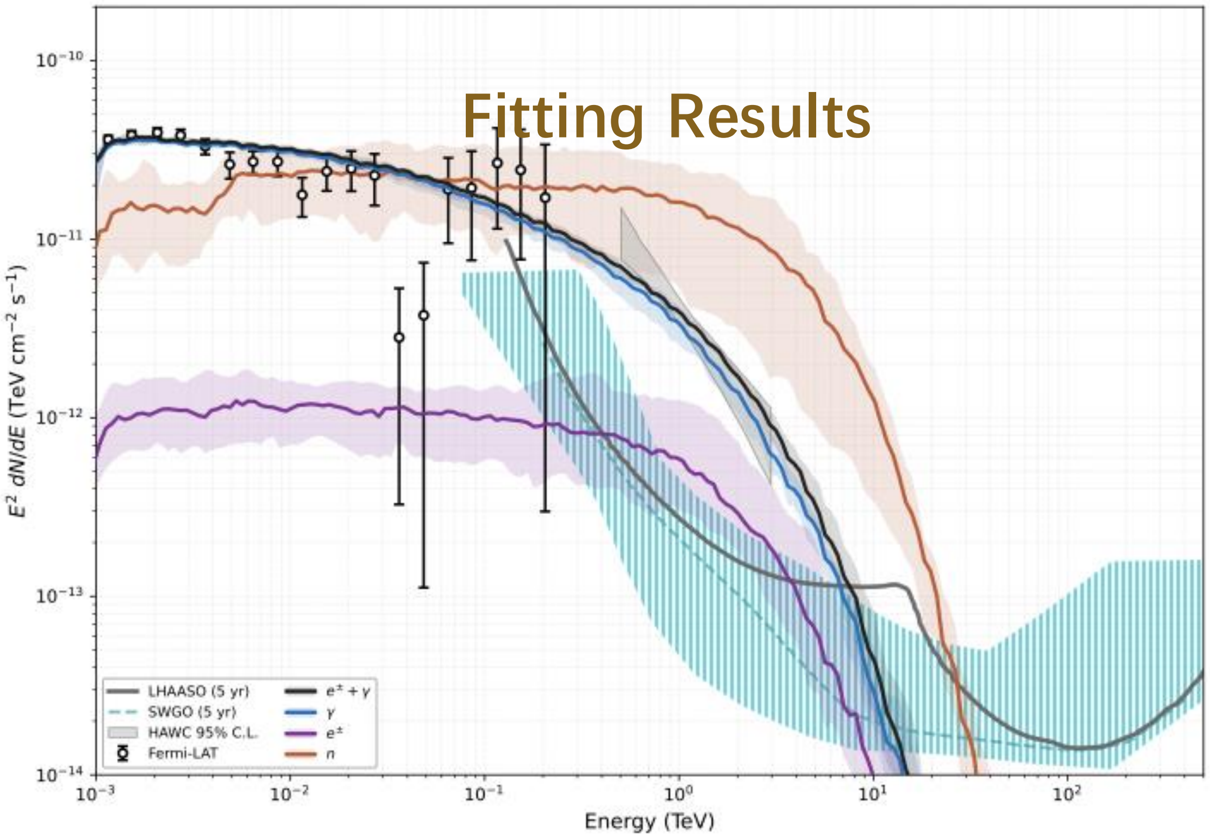

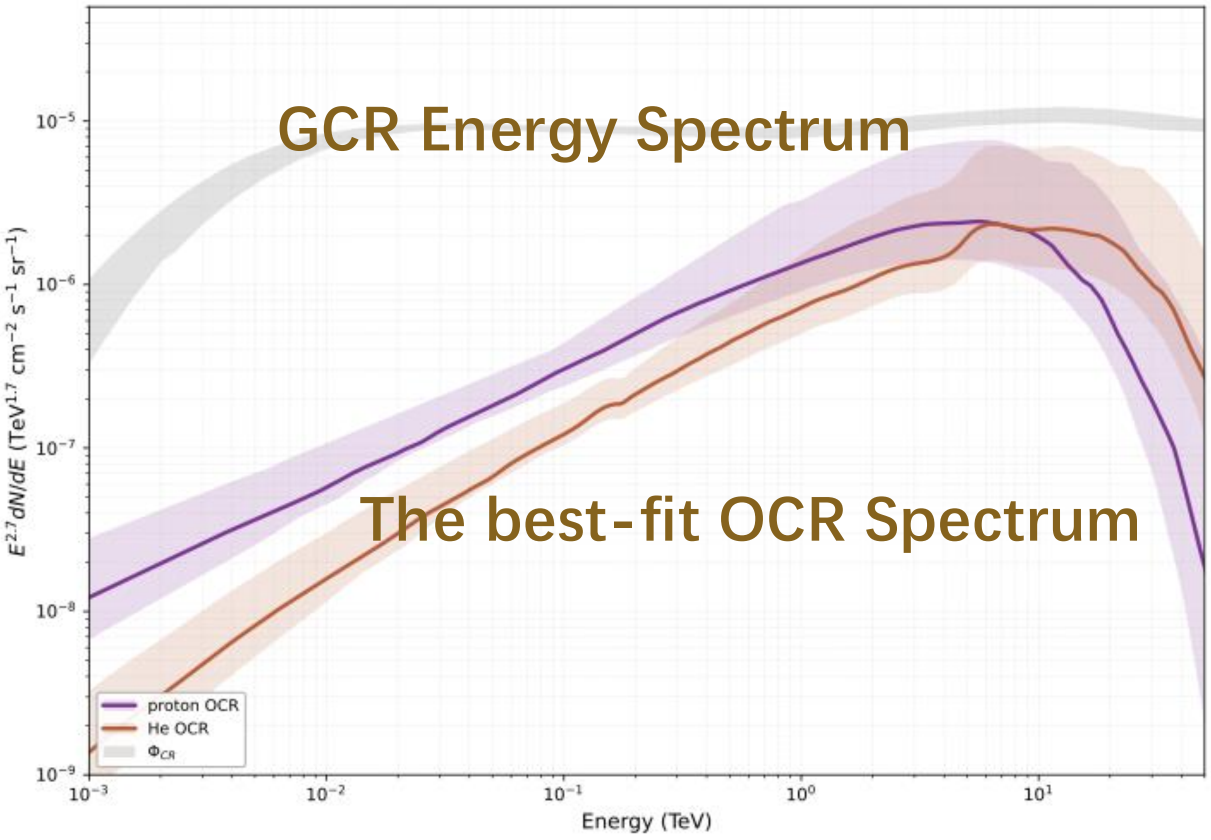

Across 38 physically allowed models

The ratio of $e^{\pm}$

?

VLAST Pan, X. *et al. NUCL SCI TECH* **35**, 149 (2024).
HERD collaboration. *J. Phys.: Conf. Ser.* **3053**, 012001 (2025).

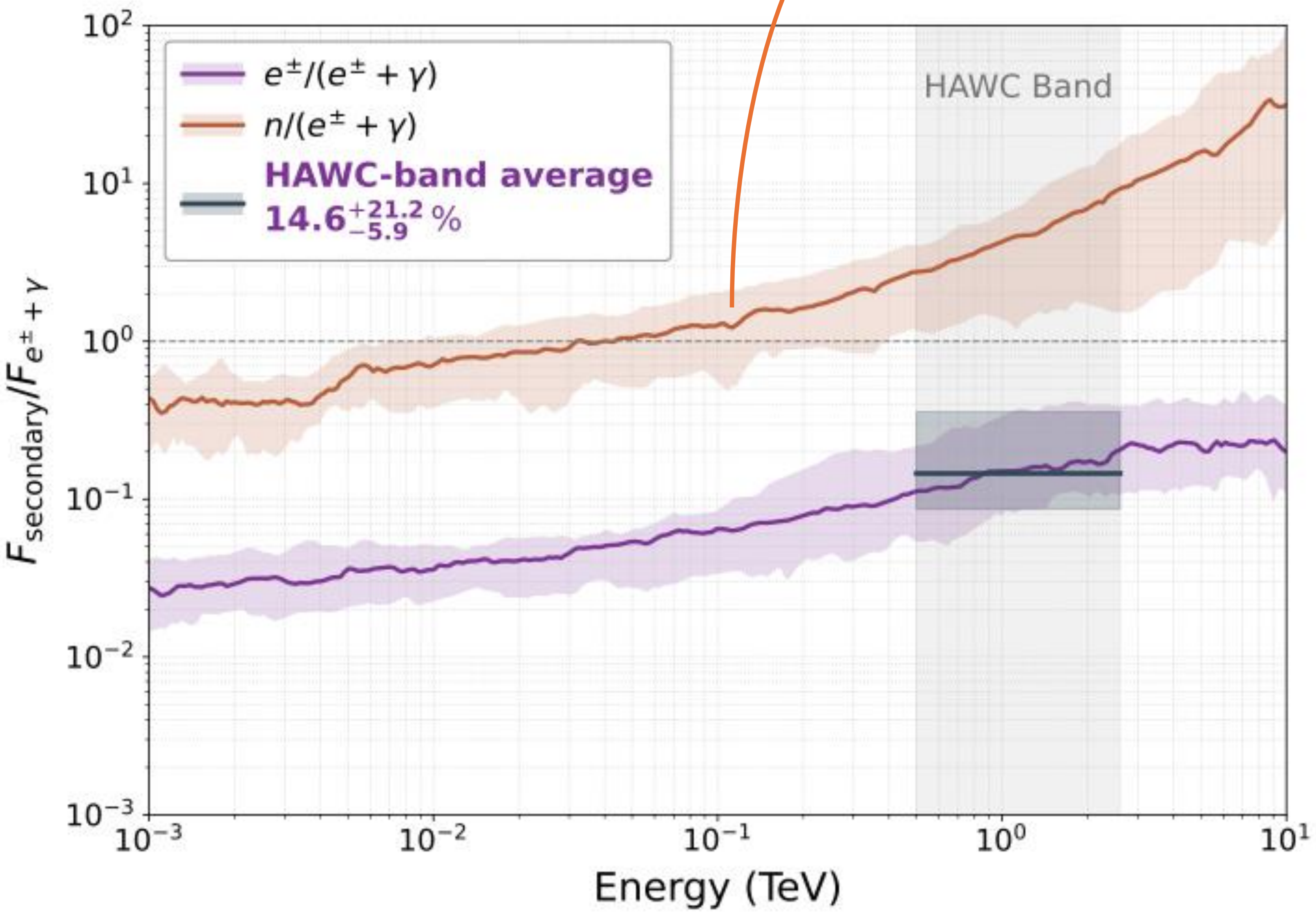

- secondary $e^{\pm}$ contribute a median fraction of **14.6%** to the HAWC-band gamma-like signal, with a central 68% model range of **8.6%-35.7%**
- Possibly the only observable astrophysical source of TeV **neutrons**.

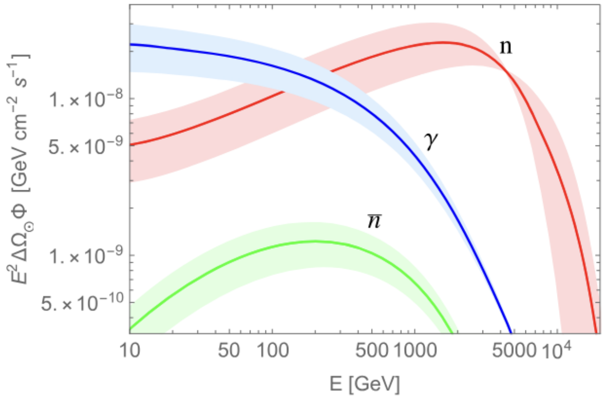

Gutiérrez, etc *ApJ* **941**, 86 (2022).

Morphology

PoS(ICRC2025) 1291 (2025). doi:10.22323/1.501.1291.

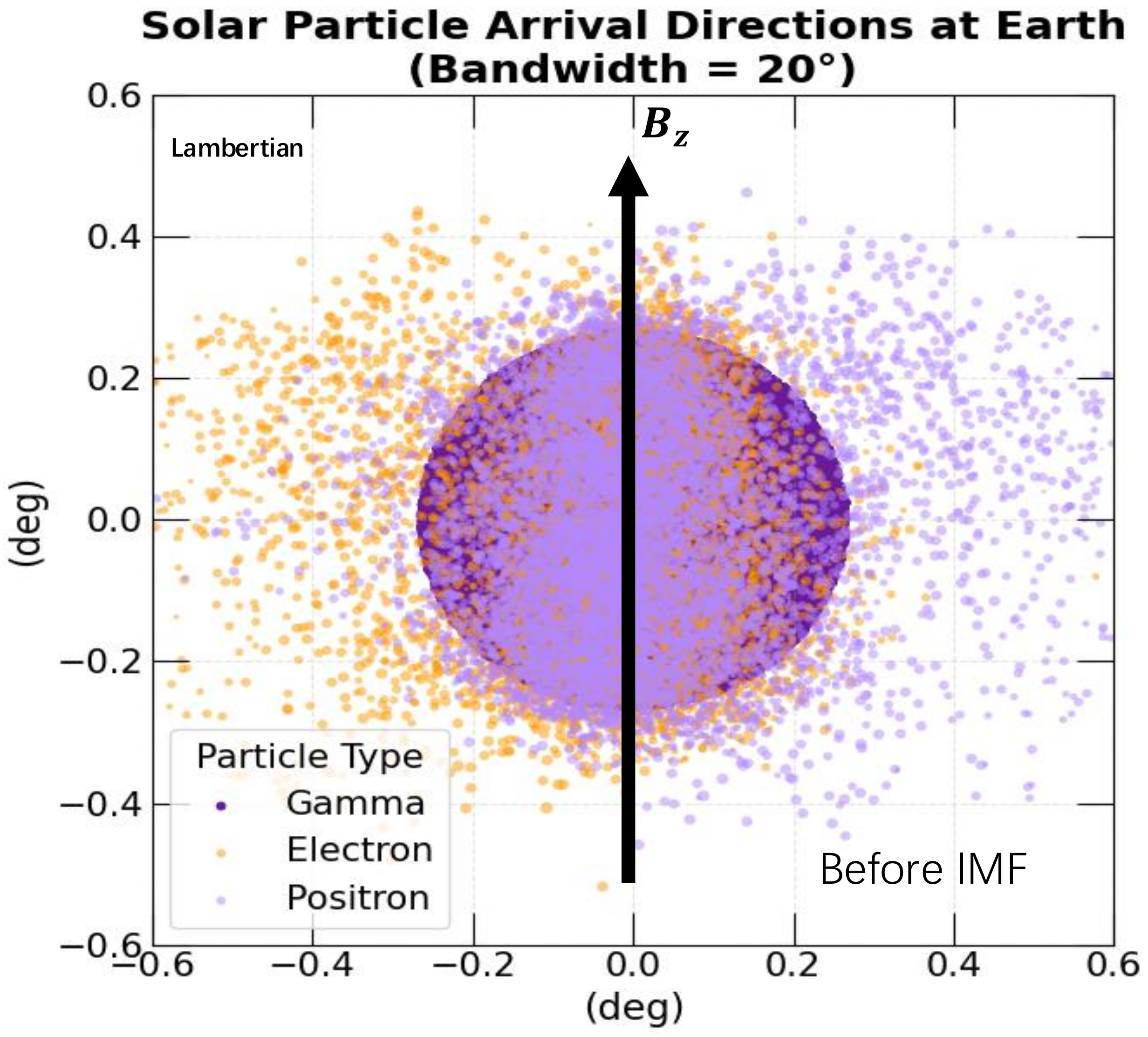

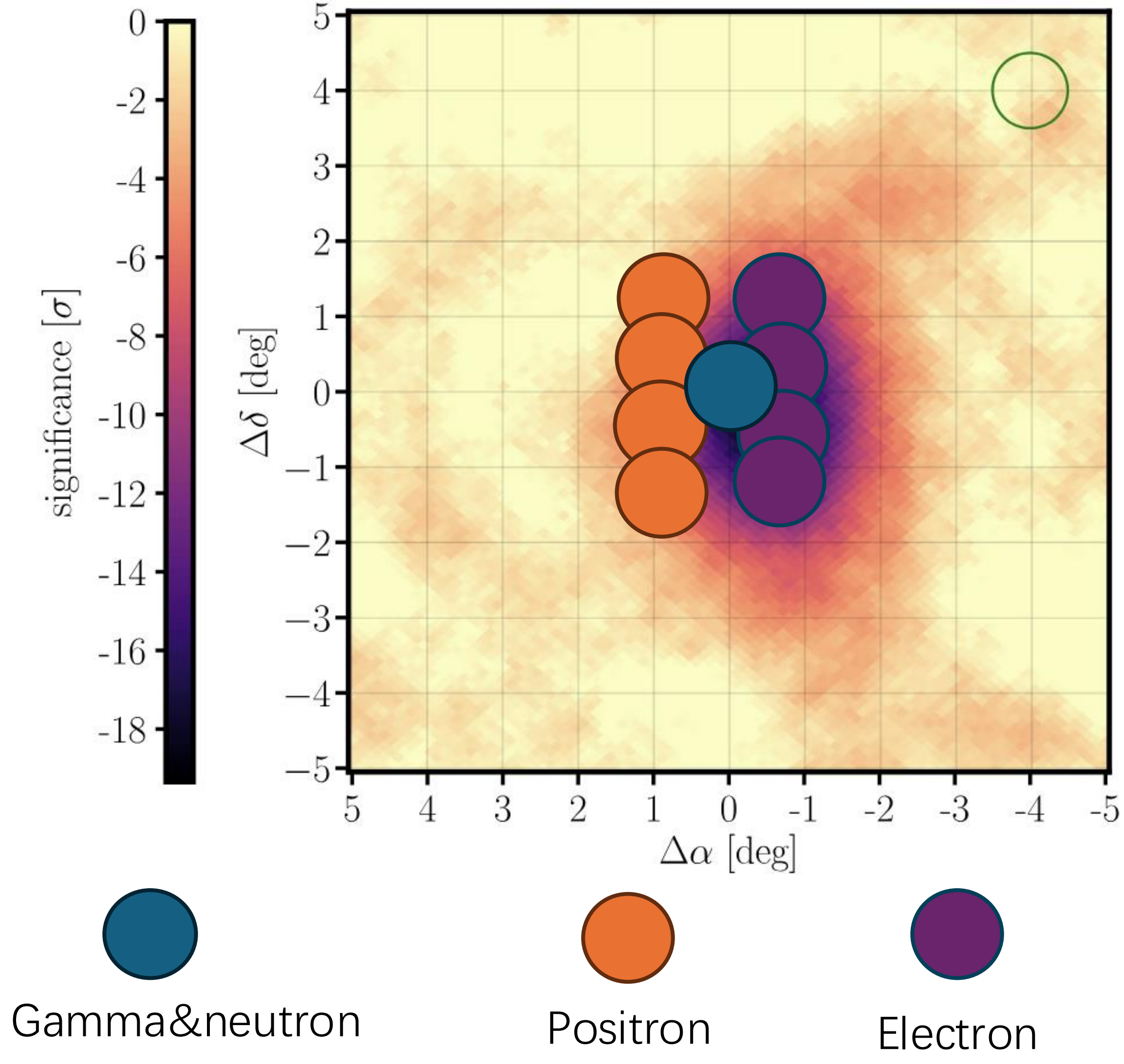

Results

- We simulated and successfully fitted the Fermi and HAWC observations of solar gamma rays, and inferred the energy spectrum of the outward-deflected cosmic rays at the solar surface.

- Across 38 physically allowed models, secondary $e^{\pm}$ contribute a median fraction of **14.6%** to the HAWC-band gamma-like signal, with a central 68% model range of **8.6%-35.7%**).

- We predicted the energy spectra of solar secondary electrons, positrons, and neutrons (Possibly the only observable astrophysical source of TeV **neutrons**) at Earth. These signals are expected to be detected by detectors such as LHAASO ($e^{\pm}$) and Fermi, VLAST, HERD (**neutrons**) in future.

References and Acknowledgements

1. Griffith, S., Beacom, J. F., Li, J.-T. & Peter, A. H. G. Angular Distribution of Gamma Rays Produced in Proton-Proton Collisions. *Phys. Rev. D* **112**, 043009 (2025).
2. Aharonian, F. *et al.* Observation of the Crab Nebula with LHAASO-KM2A − a performance study *. *Chinese Phys. C* **45**, 025002 (2021).
3. Aharonian, F. *et al.* Performance of LHAASO-WCDA and observation of the Crab Nebula as a standard candle *. *Chinese Phys. C* **45**, 085002 (2021).
4. Albert, A. *et al.* Discovery of Gamma Rays from the Quiescent Sun with HAWC. *Phys. Rev. Lett.* **131**, 051201 (2023).
5. Li, Z., Ng, K. C. Y., Chen, S., Nan, Y. & He, H. Simulating gamma-ray production from cosmic rays interacting with the solar atmosphere in the presence of coronal magnetic fields. Preprint at https://doi.org/10.48550/arXiv.2009.03888 (2024).
6. Vinyoles, N. *et al.* A New Generation of Standard Solar Models. *ApJ* **835**, 202 (2017).
7. Gutiérrez, M., Masip, M. & Muñoz, S. The Solar Disk at High Energies. *ApJ* **941**, 86 (2022).
8. Fargion, D. *et al.* Over-abundant gamma-like signals around Solar disk shadows by twin bent and smeared muon and electron pairs secondaries, versus rare local TeV gamma. in *Proceedings of 39th International Cosmic Ray Conference — PoS(ICRC2025)* 1291 (2025). doi:10.22323/1.501.1291.
9. Pan, X. *et al.* Simulation study of performance of the Very Large Area gamma-ray Space Telescope. *NUCL SCI TECH* **35**, 149 (2024).
10. Serini, D. & HERD collaboration. HERD: an innovative detector to expand energy limits in direct detection of cosmic rays. *J. Phys.: Conf. Ser.* **3053**, 012001 (2025).

The works of the CUHK group are supported by Croucher foundation, RGC grants (24302721,14305822, 14308023), NSFC/RGC joint research scheme(N CUHK456/22), NSFC grant 12322517, and various CUHK internal grants.

Thanks!

Backup slides

G4Solar Simulation

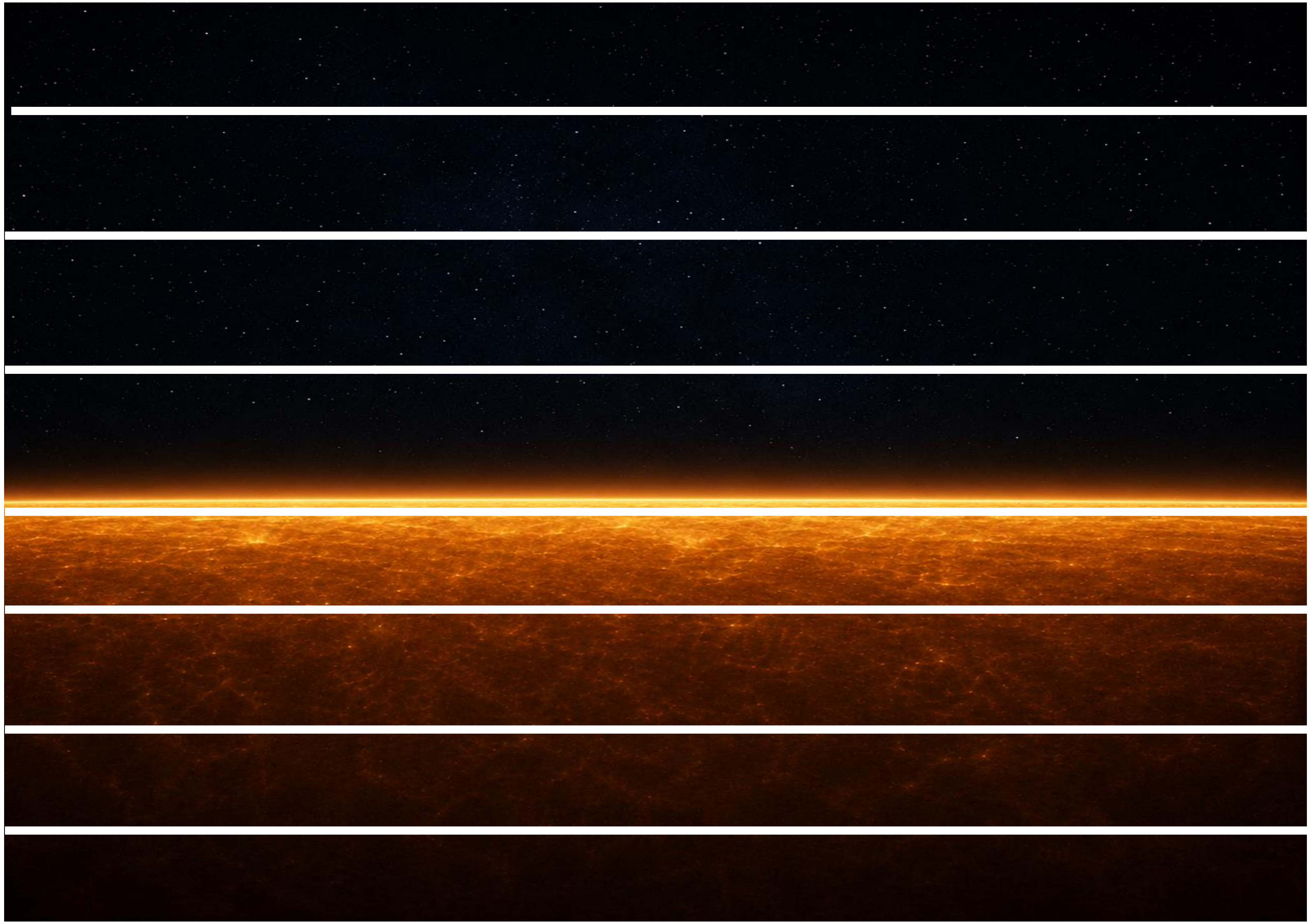

2000km

chromosphere

1500km

1000km

500km

photosphere

0km

-500 km

-1000 km

Sub-photosphere

-1500 km

-2000 km

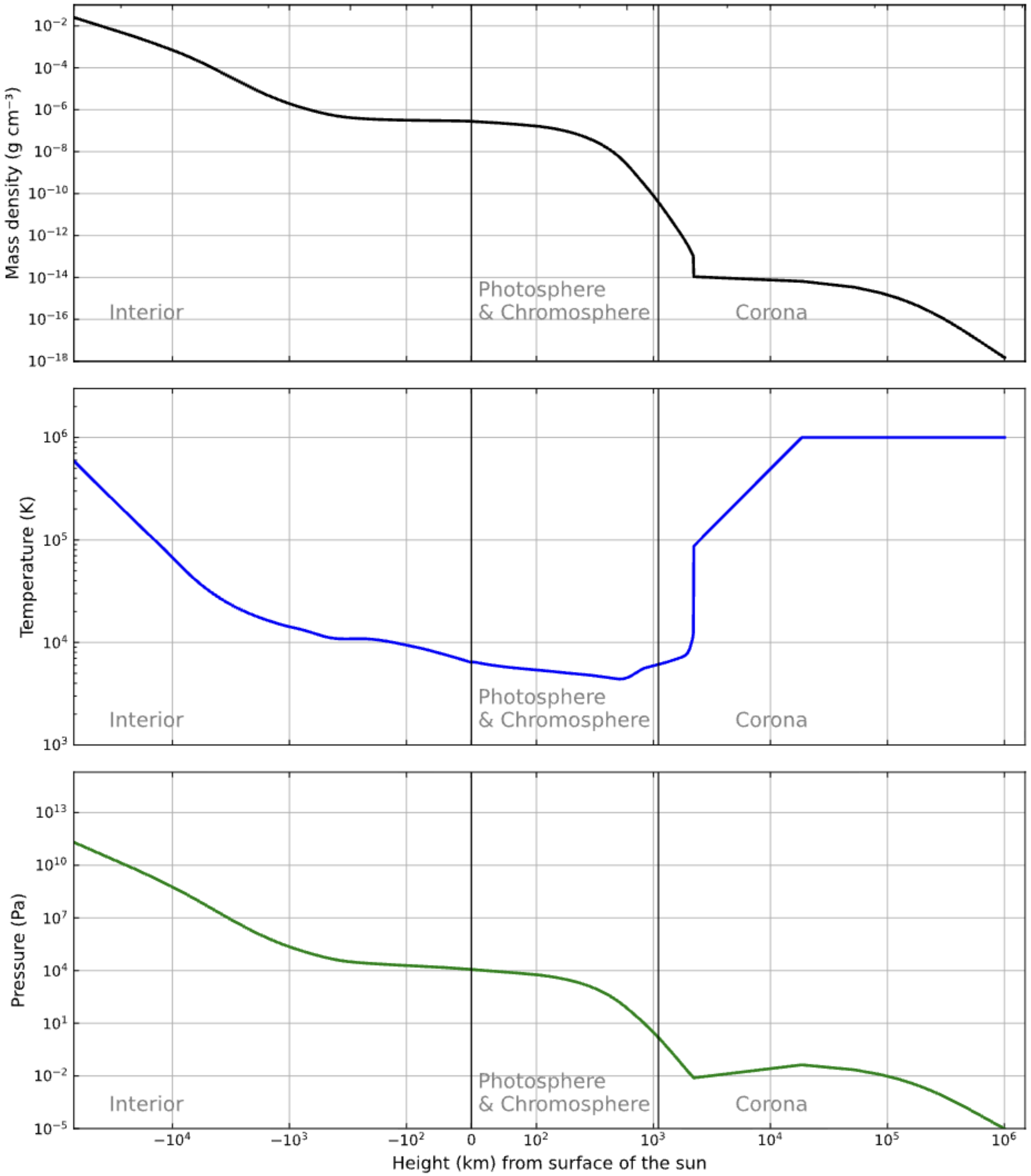

ApJ **835**, 202 (2017).

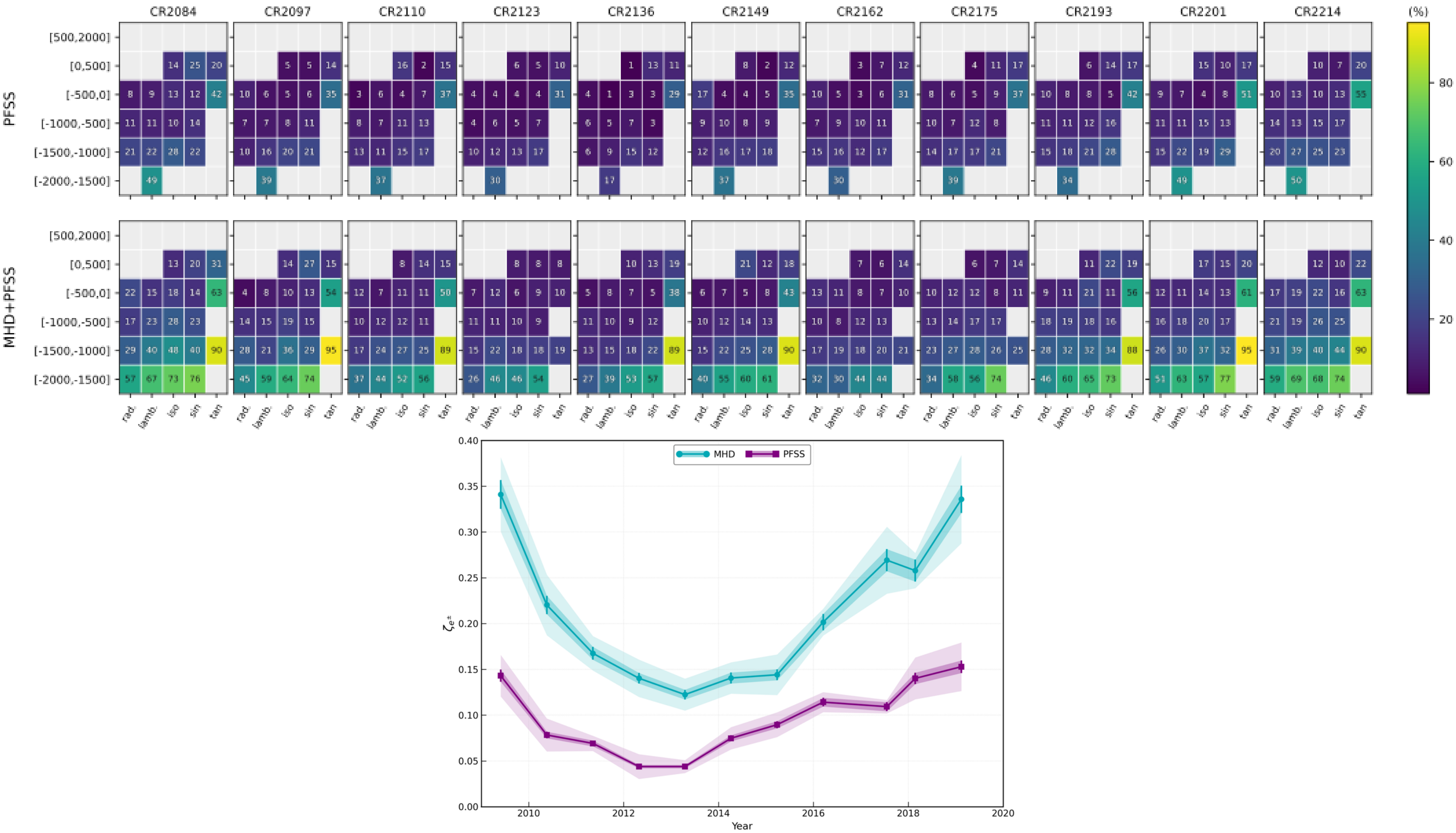

CR2084
CR2097
CR2110
CR2123
CR2136
CR2149
CR2162
CR2175
CR2193
CR2201
CR2214
(%)
PFSS
MHD+PFSS
[500,2000]
[0,500]
[-500,0]
[-1000,-500]
[-1500,-1000]
[-2000,-1500]
rad.
lamb.
iso
sin
tan
20
40
60
80
MHD
PFSS
$\zeta_{e^{\pm}}$
Year
0.00
0.05
0.10
0.15
0.20
0.25
0.30
0.35
0.40
2010
2012
2014
2016
2018
2020

Cooling of e+ e-

Can electrons/positron escape from the sun?

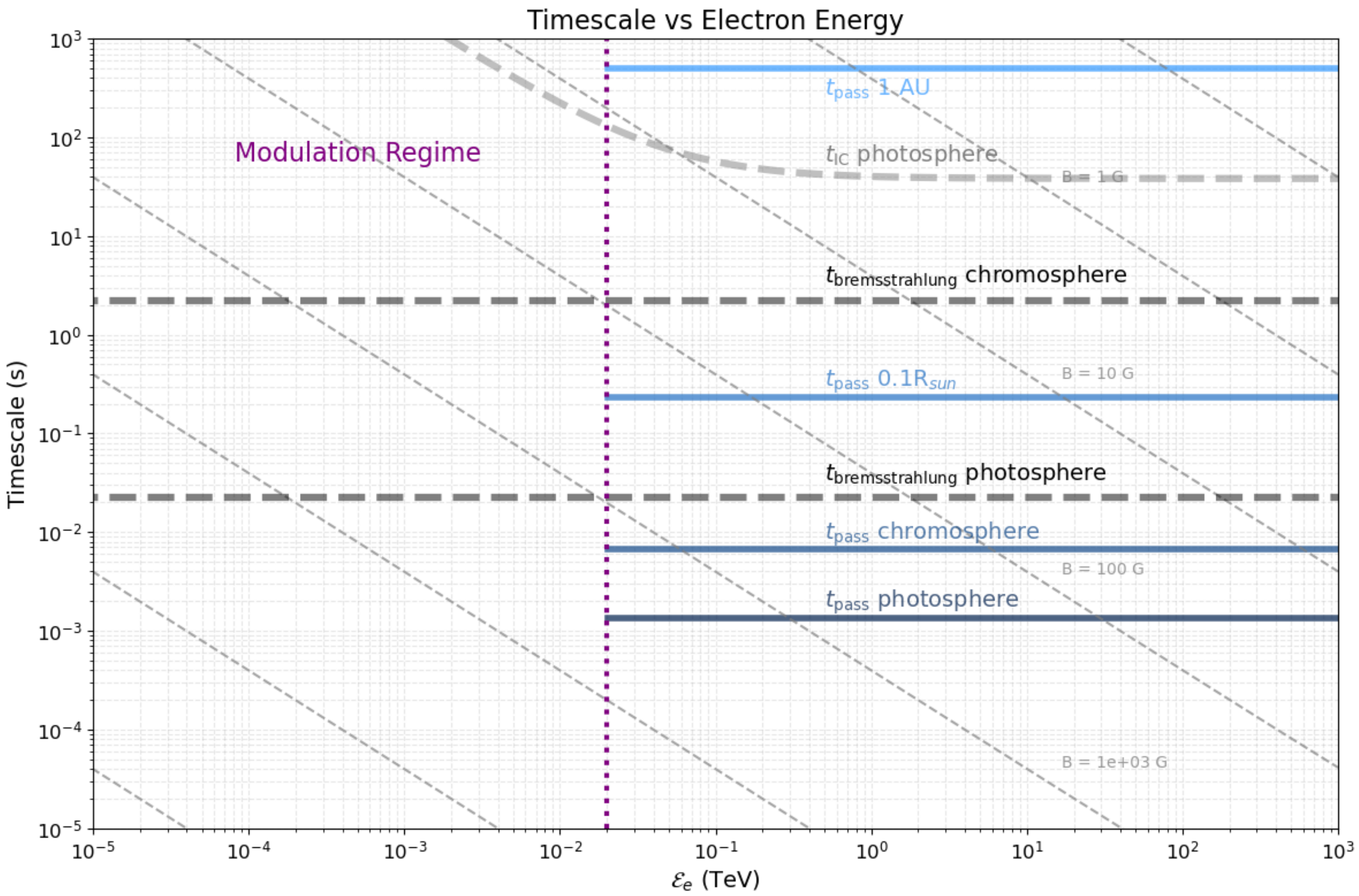

<1PeV: photosphere
chromosphere

<10TeV 1.1*R_sun
1AU

$$P_{\text{surv}} \simeq \begin{cases} 0.73, & 1\text{ GeV} \\ 0.95, & 10\text{ GeV} \\ 0.995, & 100\text{ GeV} \\ 0.9995, & 1\text{ TeV}. \end{cases}$$

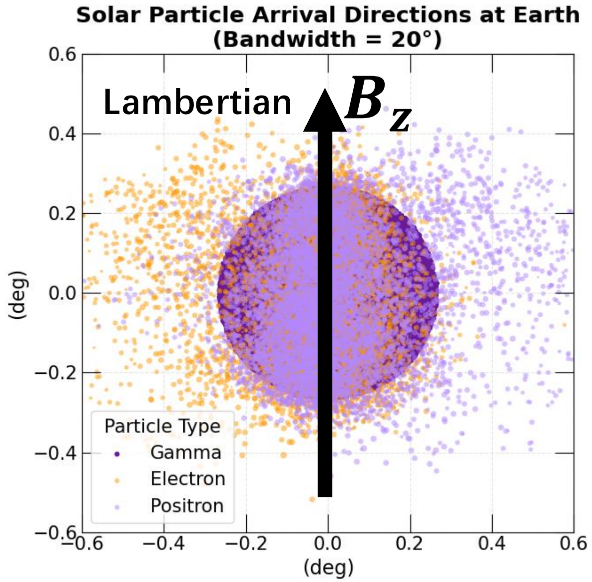
Solar Particle Arrival Directions at Earth
(Bandwidth = 20°)
Lambertian
B_z
Particle Type
Gamma
Electron
Positron
(deg)
(deg)
0.6
0.4
0.2
0.0
−0.2
−0.4
−0.6

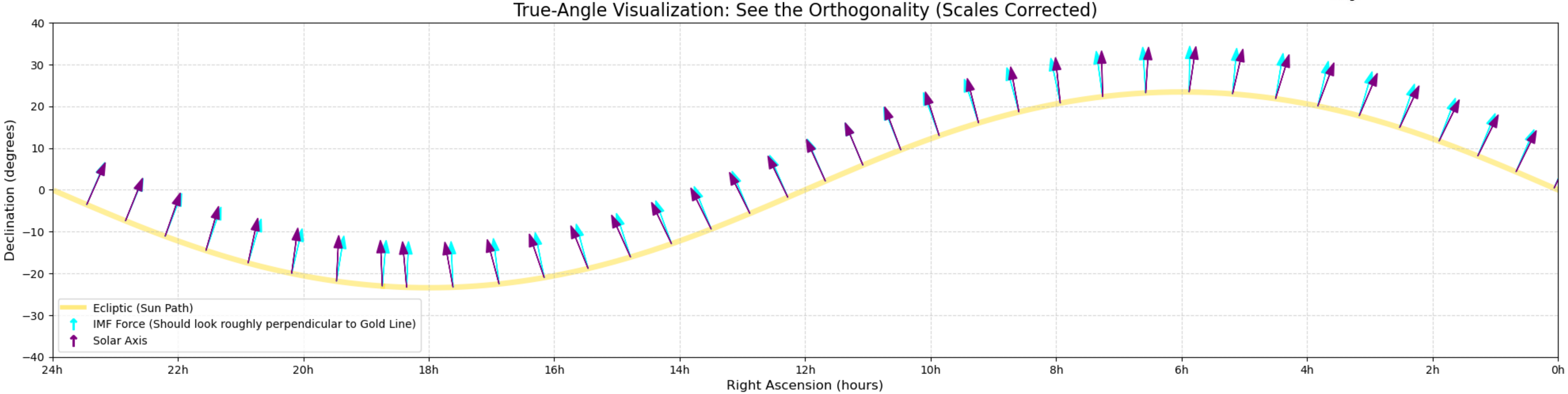
True-Angle Visualization: See the Orthogonality (Scales Corrected)
Declination (degrees)
Right Ascension (hours)
Ecliptic (Sun Path)
IMF Force (Should look roughly perpendicular to Gold Line)
Solar Axis
24h
22h
20h
18h
16h
14h
12h
10h
8h
6h
4h
2h
0h
40
30
20
10
0
−10
−20
−30
−40

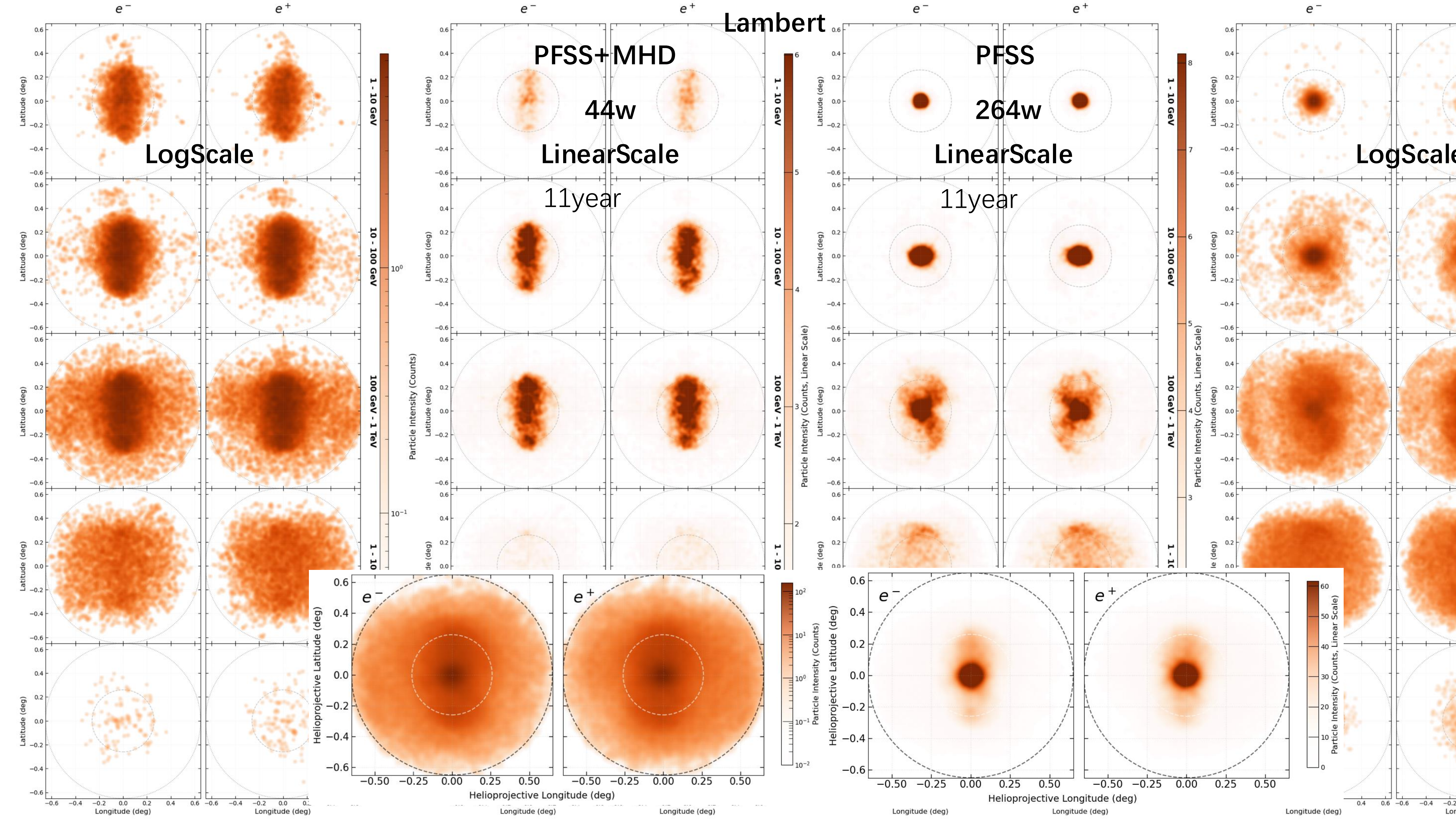
Lambert
PFSS+MHD
44w
LinearScale
11year
PFSS
264w
LinearScale
11year
LogScale
LogScale
e^-
e^+
1 - 10 GeV
10 - 100 GeV
100 GeV - 1 TeV
Particle Intensity (Counts)
Particle Intensity (Counts, Linear Scale)
Latitude (deg)
Longitude (deg)
Helioprojective Latitude (deg)
Helioprojective Longitude (deg)

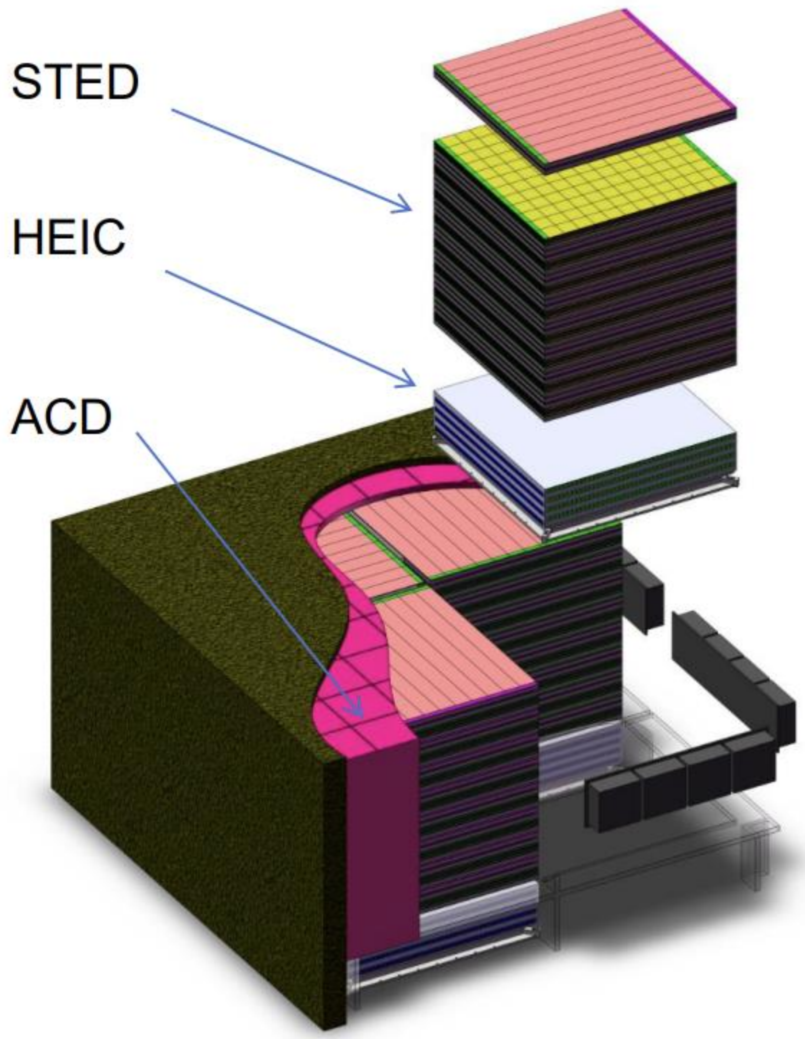

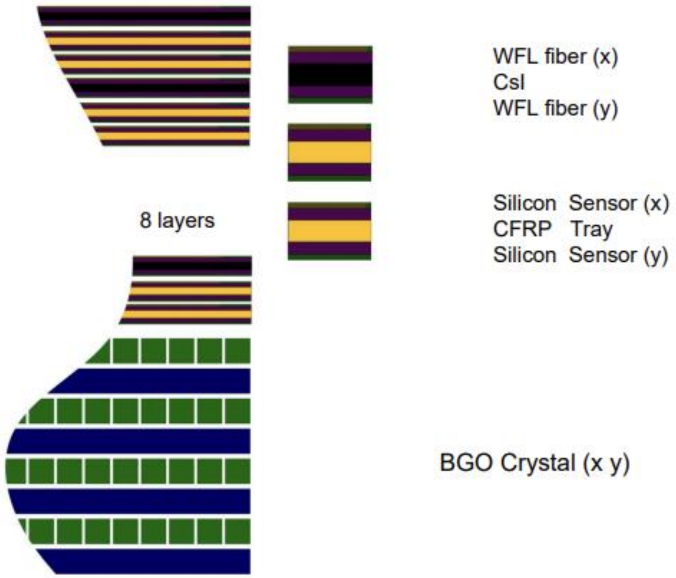

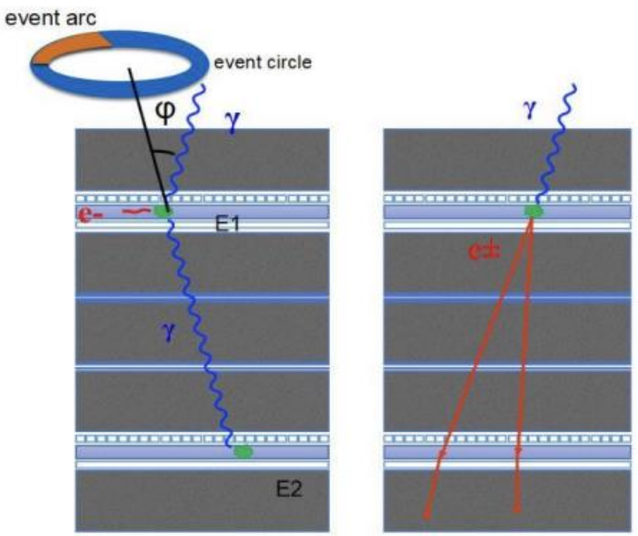

no charge + hadronic shower + direction toward Sun